






The influence of variations in ocular biometric and optical parameters on differences in refractive error

Arezoo Farzanfar^{1,2}  | Veronica Lockett-Ruiz³  | Rafael Navarro³  | Carina Koppen^{1,2}  | Jos J. Rozema^{1,2} 

¹Visual Optics Lab Antwerp (VOLANTIS), Faculty of Medicine and Health Sciences, Antwerp University, Wilrijk, Belgium

²Department of Ophthalmology, Antwerp University Hospital, Edegem, Belgium

³INMA, Consejo Superior de Investigaciones Científicas & Universidad de Zaragoza, Zaragoza, Spain

Correspondence

Jos J. Rozema, University of Antwerp, Wilrijk, Belgium.

Email: jos.rozema@uantwerpen.be

Funding information

Horizon 2020 Framework Programme, Grant/Award Number: 956720

Abstract

Purpose: To present a paraxial method to estimate the influence of variations in ocular biometry on changes in refractive error (S) at a population level and apply this method to literature data.

Methods: Error propagation was applied to two methods of eye modelling, referred to as the simple method and the matrix method. The simple method defines S as the difference between the axial power and the whole-eye power, while the matrix method uses more accurate ray transfer matrices. These methods were applied to literature data, containing the mean ocular biometry data from the SyntEyes model, as well as populations of premature infants with or without retinopathy, full-term infants, school children and healthy and diabetic adults.

Results: Applying these equations to 1000 SyntEyes showed that changes in axial length provided the most important contribution to the variations in refractive error (57%–64%), followed by lens power/gradient index power (16%–31%) and the anterior corneal radius of curvature (10%–13%). All other components of the eye contributed <4%. For young children, the largest contributions were made by variations in axial length, lens and corneal power for the simple method (67%, 23% and 8%, respectively) and by variations in axial length, gradient lens power and anterior corneal curvature for the matrix method (55%, 21% and 14%, respectively). During myopisation, the influence of variations in axial length increased from 54.5% to 73.4%, while changes in corneal power decreased from 9.82% to 6.32%. Similarly, for the other data sets, the largest contribution was related to axial length.

Conclusions: This analysis confirms that the changes in ocular refraction were mostly associated with variations in axial length, lens and corneal power. The relative contributions of the latter two varied, depending on the particular population.

KEYWORDS

error propagation, ocular biometry, refractive error, SyntEyes model

INTRODUCTION

Early studies^{1–4} established that ocular biometric parameters can vary widely between individuals and that strong correlations exist between these parameters, in both emmetropes and ametropes. However, as refractive errors are caused by a mismatch between these parameters, different correlations are found in each refractive

group.⁵ In particular, the influence of variations in axial length on refractive error has been clearly established,^{6–8} but the importance of differences in corneal power, for example, is less clear, with some studies confirming^{9–11} and others^{12,13} not showing a significant influence. Similarly, while some reports have shown that the anterior chamber depth (ACD) is generally deeper in myopes than in hypermetropes,^{10,11,14} other authors were unable

This is an open access article under the terms of the [Creative Commons Attribution-NonCommercial-NoDerivs](https://creativecommons.org/licenses/by-nc-nd/4.0/) License, which permits use and distribution in any medium, provided the original work is properly cited, the use is non-commercial and no modifications or adaptations are made.

© 2024 The Authors. *Ophthalmic and Physiological Optics* published by John Wiley & Sons Ltd on behalf of College of Optometrists.

to confirm this finding.^{15,16} Though seemingly contradictory, this discrepancy between studies arises from differences in the range of refractive error being considered. Consequently, to understand the variations within a population's refractive error, one must know the variability of its ocular biometry.

Although these observations are for adult eyes, they are especially important in developing or pathological eyes, where the relative contributions of the biometric components will be somewhat different from those found in adults. The newborn eye, for example, undergoes marked biometric changes during eye growth^{17,18} that are interconnected in a complex way that has to be just right to achieve emmetropia.¹⁹ One example is the dynamic adaptation of crystalline lens power to axial length during homeostatic eye growth, the failure of which may lead to the development of myopia.^{20,21} But just as there are large variations in biometry between individuals of any age,^{22,23} the method by which the adult refractive error is reached is unique for each eye.^{22,24} In other words, the refractive state of an eye at any time is the result of its growth history, which is typically not known during clinical examination. It is therefore more practical to study the origins of refractive error at a population level, while keeping in mind the specific biometric variability.

To this end, we propose an alternative approach to investigate the contributions of and interactions between ocular biometric parameters to the variations in refractive error using the principles of error propagation. Similar methods have been used to identify successfully sources affecting the outcome of cataract surgery²⁵⁻²⁷ and to determine how minor changes in ocular biometry affect the overall refractive error.²⁸ This analysis is implemented as either a set of two lenses, representing the cornea and the lens, or as ray transfer matrices.²⁹ After an initial assessment of the method using synthetic test data, the method was applied to biometric data derived from the literature to determine how the ocular components contribute to the refractive errors of children at different ages, as well as adults, full-term infants, premature infants with or without retinopathy of prematurity (ROP) and adults with diabetes.³⁰⁻³⁵

METHODS

Error propagation

Error propagation is a well-known method used in engineering to estimate the compounded uncertainty of a parameter f that is calculated from several other parameters x_1, \dots, x_N , each with an uncertainty $\Delta x_1, \dots, \Delta x_N$. Typically, these uncertainties are measurement errors or the standard deviation of the population. The magnitude by which each parameter x_k influences $f(x_1, \dots, x_N)$ is then given by its uncertainty multiplied by the partial derivatives as follows³⁶:

Key points

- The distribution of the refractive error is determined by variations in the ocular dimensions, but the importance of each contribution remains unclear.
- The contribution of each individual refractive component to the refractive error can be estimated by means of error propagation.
- Variations in ocular refraction are mostly associated with axial length, lens and corneal power, but their relative contribution varied depending on the examined population.

$$\Delta f(x_1, \dots, x_N) = \sqrt{\sum_{k=1}^N \left(\frac{\partial f}{\partial x_k}\right)^2 (\Delta x_k)^2} \quad (1)$$

In the context of eye models, parameters x_k refer to axial length, corneal power, ACD, corneal thickness, lens thickness, lens power, etc., while the function f represents the spherical refractive error S . Uncertainties Δx_k represent the standard deviations of parameter x_k .

Note that the compounded uncertainty calculated using Equation (1) will likely be larger than one would find if the values for f were measured directly.³⁷ This is not a problem for the current analysis, because we are interested in the relative contributions of each x_k and Δx_k to Δf rather than the value of Δf itself. These were estimated as follows:

$$100 \times \left(\frac{\partial f}{\partial x_i}\right)^2 (\Delta x_i)^2 / \sum_{k=1}^N \left(\frac{\partial f}{\partial x_k}\right)^2 (\Delta x_k)^2 \quad (2)$$

All partial derivatives were calculated manually and validated using the MATLAB symbolic toolbox (R2022a, [mathworks.com](https://www.mathworks.com)).

Simple method

The first paraxial method to determine refractive error from ocular biometry starts from the observation that spherical refractive error S is the difference between the axial power P_{ax} and whole eye power P_{eye} . Both powers can be expanded as follows³⁸:

$$S = P_{ax} - P_{eye} = \left(\frac{n}{L - pp_{eye2}}\right) - \left(P_c + P_l - P_c \cdot P_l \cdot \frac{pp_{c2} + ACD_{tot} + pp_{l1}}{n}\right) \quad (3)$$

for which the definitions of all parameters are provided in Table 1 and Figure 1. These include clinically

TABLE 1 Overview of the biometric parameters and paraxial calculations used, derived from the Navarro eye model²⁹ and age-based regressions.³⁸

Symbol	Unit	Calculation/value	Description
<i>CCT</i>	mm	0.540	Central corneal thickness
<i>ACD</i>	mm	Measured/Taken from eye model	ACD (excl. corneal thickness)
<i>ACD_{tot}</i>	mm	Measured/Taken from eye model	ACD (incl. corneal thickness)
<i>LT</i>	mm	Measured/Taken from eye model	Lens thickness
<i>L</i>	mm	Measured/Taken from eye model	Axial length
<i>n_{air}</i>	–	1.000	Refractive index of air
<i>n_c</i>	–	1.376	Refractive index of the cornea
<i>n_s</i>	–	1.3726	Refractive index of the lens surface
<i>n_l</i>	–	Measured/Taken from eye model	Equivalent refractive index of the lens
<i>n</i>	–	1.336	Refractive index of the ocular humours
<i>r_{ca}</i>	mm	Measured/Taken from eye model	Anterior on-axis corneal radius of curvature
<i>r_{cp}</i>	mm	0.821· <i>r_{ca}</i>	Posterior on-axis corneal radius of curvature
<i>P_{ca}</i>	D	(<i>n_c - n_{air}</i>) / <i>r_{ca}</i>	Anterior corneal curvature
<i>P_{cp}</i>	D	(<i>n - n_c</i>) / <i>r_{cp}</i>	Posterior corneal curvature
<i>P_c</i>	D	<i>P_{ca} + P_{cp} - 0.001 · P_{ca} · P_{cp} · CCT / n_c</i>	Total corneal power
<i>r_{la}</i>	mm	Measured/Taken from eye model	Anterior on-axis lens radius of curvature
<i>r_{lp}</i>	mm	Measured/Taken from eye model	Posterior on-axis lens radius of curvature
<i>P_{la}</i>	D	(<i>n_l - n</i>) / <i>r_{la}</i>	Anterior lens power
<i>P_{lp}</i>	D	(<i>n - n_l</i>) / <i>r_{lp}</i>	Posterior lens power
<i>P_l</i>	D	<i>P_{la} + P_{lp} - 0.001 · P_{la} · P_{lp} · LT / n_l</i>	Total lens power
<i>P_s</i>	D	<i>P_{la} + P_{lp} - 0.001 · P_{la} · P_{lp} · LT / n_s</i>	Surface power of the lens
<i>P_G</i>	D	<i>P_l - P_s</i>	Contribution of gradient-index (GRIN) structure to lens power
<i>pp_{c2}</i>	mm	-0.057	Position of second corneal principal point ^a
<i>pp_{l1}</i>	mm	5.809-0.697·exp(-0.211·Age)	Position of first corneal principal point ^a
<i>pp_{eye2}</i>	mm	0.392·exp(-0.181·Age)-2.4·10 ⁻³ ·Age+2.093	Position of second ocular principal point ^a

Note: Age in years.

Abbreviations: ACD, anterior chamber depth; D, dioptres.

^aWith respect to the anterior corneal apex.

available parameters, such as axial length *L*, total corneal power *P_c* and total anterior chamber depth (*ACD_{tot}*), as well as the estimated refractive index of the humours *n*. The principal plane positions (*pp_{eye2}*, *pp_{c2}* and *pp_{l1}*) are more difficult to determine clinically; so instead, age-based regressions were used.³⁸ Because age is not a variable in the error propagation, these age-based principal plane positions will behave as constants in the analysis. The refractive index *n*, determined by the salt and protein concentrations in the humours, presents little variation between individuals.^{39,40}

The formulas needed to calculate the error propagation can be derived by applying Equation (1) to the parameters in Equation (3). Considering the three principal points as constants, this gives the following:

with

$$\frac{\partial S}{\partial L} = - \frac{n}{(L - pp_{eye2})^2}$$

$$\frac{\partial S}{\partial P_l} = -1 + P_c \cdot \frac{pp_{c2} + ACD_{tot} + pp_{l1}}{n}$$

$$\frac{\partial S}{\partial P_c} = -1 + P_l \cdot \frac{pp_{c2} + ACD_{tot} + pp_{l1}}{n}$$

$$\frac{\partial S}{\partial ACD_{tot}} = P_c \cdot P_l / n$$

$$\frac{\partial S}{\partial n} = \frac{1}{L - pp_{eye2}} - \frac{P_l P_c (ACD_{tot} + pp_{c2} + pp_{l1})}{n^2}$$

$$\Delta S = \sqrt{\left(\frac{\partial S}{\partial L}\right)^2 (\Delta L)^2 + \left(\frac{\partial S}{\partial P_c}\right)^2 (\Delta P_c)^2 + \left(\frac{\partial S}{\partial P_l}\right)^2 (\Delta P_l)^2 + \left(\frac{\partial S}{\partial ACD_{tot}}\right)^2 (\Delta ACD_{tot})^2 + \left(\frac{\partial S}{\partial n}\right)^2 (\Delta n)^2} \tag{4}$$

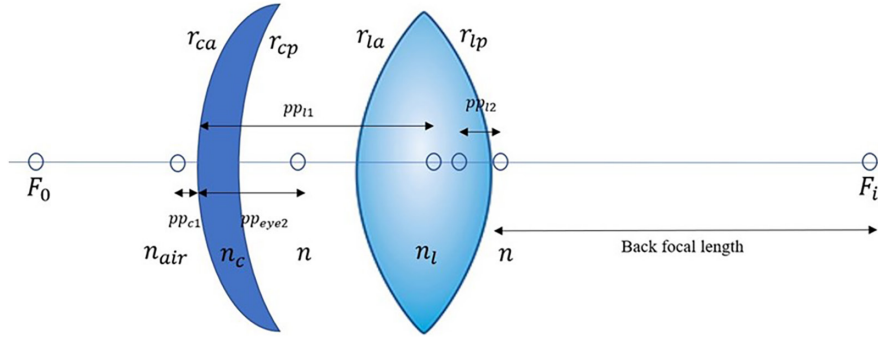


FIGURE 1 Principal planes and focal lengths, with r_{ca} and r_{cp} the anterior and posterior corneal radii of curvature, r_{la} and r_{lp} the anterior and posterior lenticular radii of curvature, n_{air} , n_c , n and n_l the refractive indices of the air, cornea, ocular humours and the lens, and pp_{c1} , pp_{l1} and pp_{eye2} the positions of the first cornea, first lenticular and second ocular principal points with respect to the corneal apex.

These expressions are used for the simple method estimate of the influence of biometric variations on the changes in S .

Matrix method

One can also describe the eye in the form of a paraxial ray transfer matrix M_{eye} ²⁹ of which the constituent equations can be filled into an error propagation analysis. This method is more accurate than the previous one but requires more parameters, such as the corneal and lenticular radii of curvature, the gradient index power of the lens, the refractive indices and the thicknesses of all the optical media (Table 1). Matrix M_{eye} consists of four elements ABCD that represent how the position and angle of a light ray is altered when passing through the optical system, calculated through a series of matrix multiplications representing the ray's refractions and translations. Here, the contributions of the cornea and anterior chamber are incorporated in matrix M , while the gradient index of the crystalline lens requires a special matrix L_{GRIN} . Hence, the eye can be described as follows:

$$M_{eye} = L_{GRIN} \cdot M = \begin{pmatrix} L_{11} & L_{12} \\ L_{21} & L_{22} \end{pmatrix} \begin{pmatrix} M_{11} & M_{12} \\ M_{21} & M_{22} \end{pmatrix} = \begin{pmatrix} L_{11}M_{11} + L_{12}M_{21} & L_{11}M_{12} + L_{12}M_{22} \\ L_{21}M_{11} + L_{22}M_{21} & L_{21}M_{12} + L_{22}M_{22} \end{pmatrix} = \begin{pmatrix} A & B \\ C & D \end{pmatrix} \quad (5)$$

with A the dilation, B the disjucacy, C the divergence and D the divarication; each a 2×2 submatrix that alters a different aspect of the passing beams of light. A and D do not have units, while B is in units of length and C is in dioptres.⁴¹ The components of L_{GRIN} are given by the following:

$$L_{11} = 1 - LT \frac{n_s - n}{n_s r_{la}}$$

$$L_{12} = -LT \frac{n}{n_s}$$

$$L_{21} = \frac{n_s - n}{n} \left(\frac{1}{r_{la}} - \frac{1}{r_{lp}} \right) + \left(\frac{(n - n_s)^2}{n \cdot n_s r_{la} r_{lp}} LT \right) + P_G$$

$$L_{22} = 1 - LT \frac{n - n_s}{n_s r_{lp}}$$

with P_G the contribution of the gradient index to the lens power, calculated as the difference between the total lens power P_l and the lens surface power P_s (Table 1). The components of M are as follows:

$$M_{11} = \left(1 - \frac{CCT(n_c - 1)}{n_c r_{ca}} \right) \left(1 - \frac{ACD(n - n_c)}{n r_{cp}} \right) - \frac{ACD(n_c - 1)}{n r_{ca}}$$

$$M_{12} = -\frac{CCT}{n_c} \left(1 - \frac{ACD(n - n_c)}{n r_{cp}} \right) - \frac{ACD}{n}$$

$$M_{21} = \frac{n_c - 1}{n r_{ca}} \left(1 - \frac{CCT(n - n_c)}{n_c r_{cp}} \right) + \frac{n - n_c}{n r_{cp}}$$

$$M_{22} = \frac{1}{n} \left(1 - \frac{CCT(n - n_c)}{n_c r_{cp}} \right)$$

Matrix elements A and C in Equation (4) can then be used to estimate the position of the principal plane on the image side with respect to the anterior corneal apex as follows:

$$pp_{eye2} = CCT + ACD + LT + (A - 1)/C \quad (6)$$

Meanwhile, the power of the entire eye is given by the following:

$$P_{eye} = \frac{n}{f_{eye2}} = n \cdot C \quad (7)$$

with f_{eye2} the focal distance on the image side. The full expressions for A and C are provided in Appendix S1.

From this, the refractive error can be calculated as follows:

$$S = P_{ax} - P_{eye} = \frac{n}{L - pp_{eye2}} - n \cdot C \tag{8}$$

$$= \frac{n}{L - CCT - ACD - LT + (A - 1)/C} - n \cdot C$$

Error propagation for this method can be achieved by filling Equation (7) into (1), resulting in the following:

$$\Delta S = \sqrt{\begin{aligned} & \left(\frac{\partial S}{\partial L}\right)^2 (\Delta L)^2 + \left(\frac{\partial S}{\partial P_G}\right)^2 (\Delta P_G)^2 + \left(\frac{\partial S}{\partial r_{ca}}\right)^2 (\Delta r_{ca})^2 + \left(\frac{\partial S}{\partial ACD}\right)^2 (\Delta ACD)^2 + \left(\frac{\partial S}{\partial LT}\right)^2 (\Delta LT)^2 \\ & + \left(\frac{\partial S}{\partial r_{lp}}\right)^2 (\Delta r_{lp})^2 + \left(\frac{\partial S}{\partial r_{la}}\right)^2 (\Delta r_{la})^2 + \left(\frac{\partial S}{\partial n_s}\right)^2 (\Delta n_s)^2 + \left(\frac{\partial S}{\partial r_{cp}}\right)^2 (\Delta r_{cp})^2 \\ & + \left(\frac{\partial S}{\partial n}\right)^2 (\Delta n)^2 + \left(\frac{\partial S}{\partial n_c}\right)^2 (\Delta n_c)^2 + \left(\frac{\partial S}{\partial CCT}\right)^2 (\Delta CCT)^2 \end{aligned}} \tag{9}$$

The resulting expressions of the 12 partial derivatives are lengthy and provided in Appendix S1. Expression (9) will be used for the error propagation analysis of the matrix method.

Data

To test both methods on a realistic and complete data set, a set of 1000 SyntEyes was first used; stochastically generated biometric data sets of the eye with average values and variations that match those in the general population between 20 and 60 years of age.³⁰ Since SyntEyes provide all parameters required for either error propagation method, they form an ideal demonstration platform for these methods before applying them to clinical data.

Next, several data sets from the literature were considered. The first, from Mutti et al.,³¹ provides longitudinal biometry data for a group of children between 3 months and 6.5 years of age, allowing an understanding of changes in the contributions during emmetropisation and early homeostasis. As this data set provides information for both the lenticular radii of curvature and refractive index, both error propagation methods may be applied. A second data set, by Twelker et al.,³² is a cross-sectional cohort of school-children between 6 and 14 years of age, with an increasing prevalence of myopia. This allows the assessment of how developing myopia is reflected in the biometric changes. Here, the biometric data were averaged over the separated values for boys and girls that were provided.

An additional analysis compared the biometric contributions to refractive error in premature infants with or without ROP, examined longitudinally between 32 and 52 weeks of postmenstrual age.³⁴ Premature eyes have shorter axial lengths, shallower anterior chambers and more highly curved corneas than those of full-term infants,⁴² differences that become more considerable as the severity of ROP increases. As the number of participants was relatively small, no analysis by ROP stage could be performed. Here, lens power was estimated using Bennett's method.^{43,44} The data of full-term infants between 0 and

3 days of age, presented by Axer-Siegel et al.,^{33,45} were also considered.

Finally, since the lenticular biometry of diabetic eyes is considerably different from that of healthy eyes,³⁵ the contributions of the ocular parameters to the refractive error of 74 participants with Type 1 diabetes were compared to those in 64 age-matched controls.

The values of all required parameters and their standard deviations are given in Appendix S2 for all data sets. Since real data sets are often incomplete and typically lack the necessary information about the refractive indices of the ocular media, the indices of the Navarro eye model⁴⁶ were used to supplement the real data where needed.

RESULTS

Test data

Applying both methods to 10 sets of 1000 SyntEyes leads to the contribution percentages shown in Table 2. The largest contributions are given by the variations in axial length L , lens power P_l and corneal power P_c for the simple method (56.87%, 31.51% and 10.30%, respectively), and by L , the contribution of the gradient-index (GRIN) structure to lens power (P_G) and the anterior corneal curvature r_{ca} for the matrix method (63.62%, 16.30%, 12.94%, respectively). The contributions of the variations in the principal plane positions using the simple method (i.e., the position of second ocular principal point (pp_{eye2}), the position of the second corneal principal point (pp_{c2}) and the position of the first corneal principal point (pp_{c1})) were very small (0.50%, 0.22% and $6.79 \cdot 10^{-5}\%$, respectively).

Children

The contributions of the biometric components shown in Figure 2 were obtained by applying both error propagation methods to the children's data from Mutti et al.³¹ Again, the largest contributions were given by the variations in axial length, lenticular and corneal power for the simple method (67%, 23% and 9%, respectively), and by the axial length, gradient lens power and the anterior corneal curvature for the matrix method (55%, 21% and 14%, respectively). The percentage estimates provided by the matrix method agreed overall with the equivalent parameters in

the simple method, albeit with higher contributions from the variations in corneal power and ACD at the expense of the contribution from axial length.

Influence of myopia

In the children's data from Twelker et al.,³² myopisation caused the contribution of axial length to increase from 54.5% to 73.4%, while the contribution from the changes in lens and corneal power decreased from 35.2% to 19.94% and from 9.82% to 6.32%, respectively (Figure 3). This suggests that during normal refractive development, the

TABLE 2 Average contribution of the variations in the individual parameters to changes in refractive error for both methods based on 10 runs of 1000 SyntEyes (symbols defined in Table 1).

Parameters	Simple method	Parameters	Matrix method
L	56.87%	L	63.62%
P_l	31.51%	P_G	16.30%
P_c	10.30%	r_{ca}	12.94%
ACD_{tot}	0.65%	ACD	3.63%
pp_{eye2}	0.50%	pp_{eye2}	–
pp_{l1}	0.22%	pp_{l1}	–
pp_{c2}	$6.79 \cdot 10^{-5}\%$	pp_{c2}	–
n	0.04%	n	0.04%
LT	–	LT	1.30%
r_{lp}	–	r_{la}	0.67%
r_{la}	–	r_{lp}	0.65%
n_s	–	n_s	0.63%
r_{cp}	–	r_{cp}	0.30%
n_c	–	n_c	0.015%
CCT	–	CCT	0.01%

Note: Standard deviations over the 10 runs were all <0.01%.

percentage contributions from the variations in ocular biometry to the changes in S are generally stable, but this is disrupted by myopisation.

Full-term and pre-term infants

The contributions from the variations in ocular biometry in pre-term infants,³⁴ both with and without ROP, using the simple method are shown in Figure 4. The curves seen in children without ROP fluctuated considerably, while the contributions from axial length and lens power were about equal. The full-term children tested by Axer-Siegel and colleagues^{33,45} showed very similar results. The fluctuations in Figure 4a are likely due to the large standard deviations resulting from the relatively small population size and the fact that the lens power was calculated rather than measured, leading to compounded uncertainty.

Diabetes

Applying the simple method to the data of healthy adults and adults with diabetes,³⁵ clear differences are seen (Figure 5). Unlike the healthy adults, for the diabetic group, lens power made a considerably larger contribution to the refractive error than the cornea. Regardless, axial length variations still provided the greatest contribution to refractive error for both of these groups.

DISCUSSION

This work applied error propagation analysis to simple and matrix representations of the eye to determine how ocular biometric differences affect the distribution of the refractive error. The SyntEyes data showed that both methods

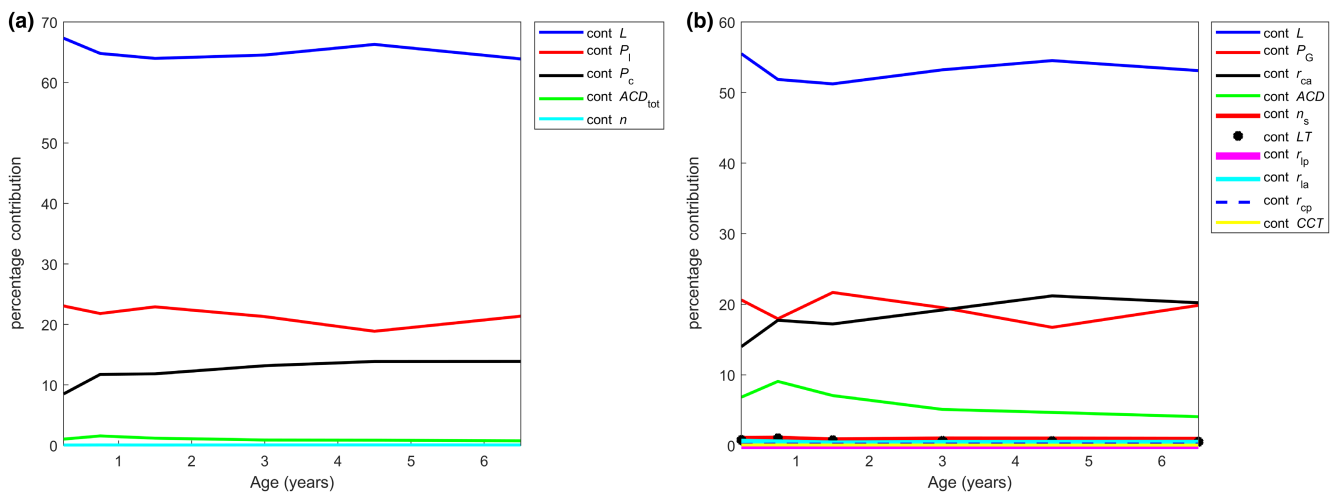


FIGURE 2 Contributions of the variations in ocular biometry to the changes in refractive error using the Mutti et al.³¹ data for: (a) the simple method and (b) the matrix method. Symbols are defined in Table 1.

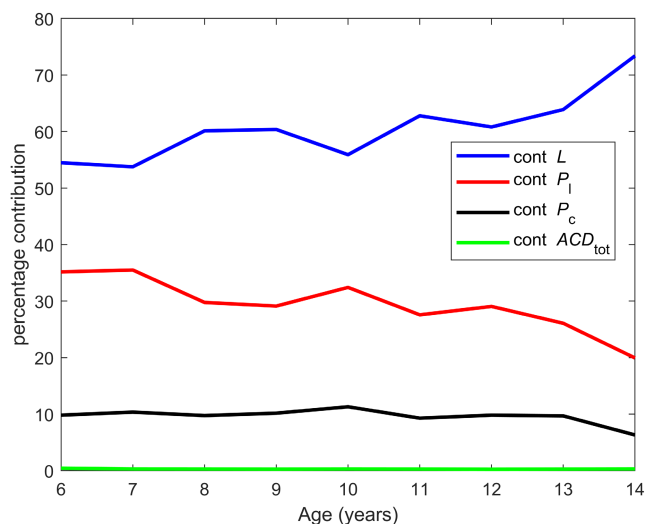


FIGURE 3 Biometric contributions to variations in refractive error from the Twelker et al.³² data using the simple method. Symbols are defined in Table 1.

assess different but related aspects of ocular biometry (Table 1), with axial length variations being responsible for about two thirds of the differences in refractive error, followed by changes in the lens power (16%–31%) and anterior corneal radius of curvature (10%–12%). This is comparable to the data for the control group of healthy adults³⁵ seen in Figure 5, which had corresponding values of 57.3%, 25.4% and 15.4%, respectively. However, the relative importance of corneal and lens powers differs between populations and data sets. To this end, both methods were applied to several data sets, including SyntEyes, which contained every parameter required, as well as clinical data sets for children and adults of different ages having a range of ocular conditions.

Applying the simple method to the longitudinal biometric data of children between the ages of 3 months and 6.5 years from Mutti et al.³¹ showed that during emmetropisation and early homeostasis, the contributions from variability in axial length, lens power and corneal curvature were comparable to those found using the simple method in adults (Figure 2a). For the matrix method, the contribution from variations in axial length was lower than for adults ($\pm 53\%$ instead of 64%), while the variations in the anterior corneal radius of curvature in young children were higher than the corneal power in adults ($\pm 20\%$ vs. 8.5%). Similar differences were seen for ACD (5%–9% vs. 3%; Figure 2b). Considered longitudinally, only very mild increases in the corneal contributions and mild decreases in the lenticular (simple method) and ACD contributions (matrix method) could be observed. This stability of the contributions is especially remarkable considering the large biometric changes that occur during this period. Myopia disrupts this stability, however, as can be seen in the longitudinal data of school age children by Twelker et al.³² With increasing myopia prevalence, the contribution of lens power gradually

decreased from 35% to 20%, while that of axial length increased from 54% to 73%. This is to be expected as myopia is typically associated with excessive axial growth.

Another group exhibiting altered refractive development are premature infants, many of whom develop ROP. Overall, pre-term infants tend to have shorter axial lengths with a shallower anterior chamber compared with full-term infants at the same gestational age.⁴⁷ In pre-term infants, this could result in high degrees of myopia later on, often driven by the cornea and lens rather than axial length, as would likely be the case in full-term individuals,⁴⁸ and ROP tends to exacerbate these effects.⁴⁹ A previous study³⁴ reported that as ROP progresses, consistent decreases in axial length and ACD are observed. The occurrence of myopia varies across different stages of ROP, suggesting a potential link. These findings highlight the complex nature of refractive development in premature infants and emphasise the need for management strategies specific to different ROP stages. Regarding the pre-term data presented by Cook et al.,³⁴ changes in axial length and lens power seemed to contribute equally to the refractive error (Figure 4). However, this result may not be reliable as the differences in ocular biometry between pre-term and full-term eyes become more manifest with age, coupled with the fact that the lens power was calculated from average data for a relatively small population compared with previous cohorts. So, while a greater contribution from lens power variations is plausible in pre-term children,⁴⁹ this observation needs to be confirmed with additional data.

Finally, the biometric variations in the diabetic group are substantially different from those in the control group, most notably with regard to the dimensions and power of the crystalline lens³⁵ and especially in those having an early onset of the disease.⁵⁰ This difference is reflected in the relative effects of variations in lens and corneal power, with a considerably larger contribution from lens power changes in diabetic eyes (Figure 5). These lenticular changes are induced, in part, by the aqueous, which undergoes a rapid drop in glucose concentration during hypoglycaemia. As the aqueous and lens interact through osmosis, an exchange of water occurs between them, depending on the patient's glycaemic state, which in turn affects the refractive index of the lens and thus the refraction of the eye.⁵¹

Similar error propagation methods have been used in previous studies, but mostly to assess how measurement errors from biometry devices affect intraocular lens (IOL) calculations and surgical outcomes.^{25–27} In those studies, the uncertainty regarding corneal power measurements formed the greatest source of error, along with estimates of the postoperative IOL position,^{25,27,28} depending on the power calculation formula being used. In a similar context, Ribeiro et al.²⁸ varied the individual dimensions of the Liou and Brennan eye model to determine corresponding changes in overall refractive error using ray tracing software. For phakic eyes measured with an optical biometer and considering the Monte Carlo process using the measurement errors of the device, variations in anterior corneal

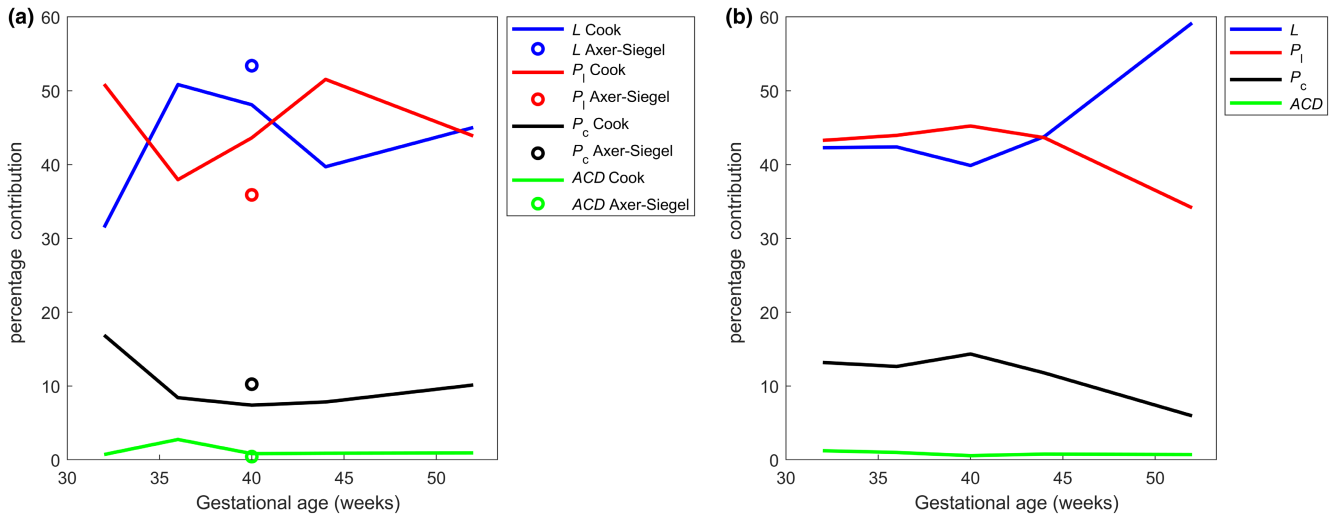


FIGURE 4 Contributions of the variations in ocular biometric components using the simple method to the changes in refractive error from the Cook et al.³⁴ data for: (a) pre-term infants without retinopathy of prematurity (ROP) and the full-term data by Axer-Siegel and colleagues^{33,45} and (b) the Cook et al. data for pre-term infants with ROP. Symbols are defined in Table 1.

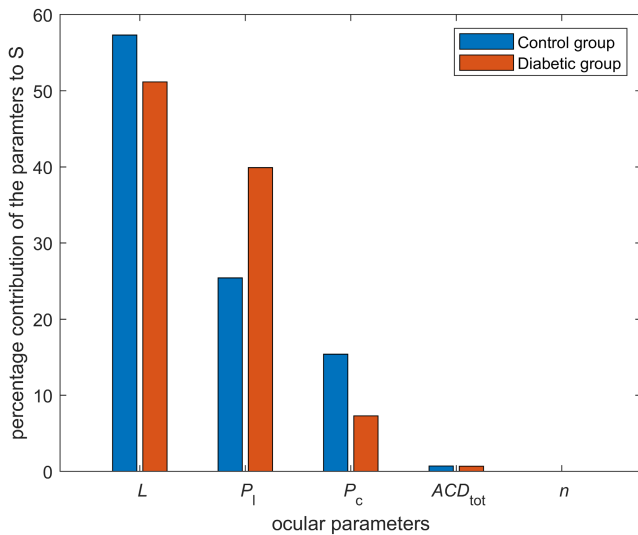


FIGURE 5 Contributions of ocular biometric components to the change in refractive error using the simple method for normal and diabetic adult groups. L is the axial length, P_1 the lens power, P_c the corneal power, ACD_{tot} , the total anterior chamber depth (including corneal thickness) and n the refractive index of the ocular humours.

asphericity most affected refractive error (36.1%), followed by the anterior radius of curvature (28.0%), corneal thickness (11.0%) and lens thickness (8.9%). Meanwhile, in pseudophakic eyes, the most important contributor by far was the postoperative ACD (76.8%). While interesting, the Ribeiro et al.²⁸ analysis did not consider the existing correlations between the biometric parameters, which would have overestimated the resulting refractive errors.⁵² Moreover, as the Monte Carlo process was considered over the range of measurement errors of an optical biometer, these percentage contributions should not be compared with the current results. Finally, in a classic study, Hirsch

and Weymouth⁵³ attempted to predict refractive error using multiple regression analysis, reporting a contribution of approximately 47% from changes in axial length, while some 24% and 7% were due to variations in corneal radius of curvature and ACD, respectively. The remaining 22% was assumed to be variations in crystalline lens curvature, refractive indices of the media and measurement errors.⁵³ These values are somewhat different from the current findings, probably because they did not include the lens power. Also, Olsen et al. used a strictly statistical approach to investigate the correlation between refractive error and ocular refractive components. Their findings revealed a significant correlation between ocular refraction and not only axial length but also lens and corneal power.¹

This analysis has some limitations. The most important is the sensitivity to large variability in standard deviations, which in turn is determined by the number of participants, and as for the IOL power analyses described above, by the measurement errors of the biometer being used. This is especially evident in the fluctuating values for calculated lens powers from the Cook et al.³⁴ and Axer-Siegel et al.^{33,45} data sets (Figure 4a), compared with the lens power values measured with a custom phakometer for a much larger data set by Mutti et al.³¹ (Figure 2). In practice, however, there are only a limited number of biometry systems on the market, having about the same level of repeatability, so using a sufficiently large data set (e.g., 50 eyes per data point) should minimise this issue. Another limitation is the unavailability of the posterior corneal radius in most of the data sets considered here, necessitating the estimate of $r_{cp} = 0.821 \cdot r_{ca}$ given in Table 1, which was previously derived³⁸ from Oculus Pentacam (pentacam.com) data of 4953 Iranian school children with a mean age of 9.74 ± 1.68 years that included both the anterior and posterior corneal radii. This method is preferred over the use of a keratometric

index, as most indices tend to overestimate the actual total power,^{54,55} and it allows more accurate thick lens calculations. Another limitation of the present study is the use of age-based regressions to estimate the position of the principal planes with the simple method, rather than their full calculation. This choice was motivated by the fact that calculation and inclusion would have led to far more complicated equations for the simple method than strictly necessary. On the other hand, the matrix method is more accurate and mathematically complete as it considers all relevant parameters, and unlike the simple method, does not make any assumptions about the principal plane position at the expense of increased complexity. Here too, a simplification with fixed principal points was considered using pp_{eye2} as a variable instead of Equation (6), but while this simplified the refractive error formula, it did not do much to simplify the partial derivatives and therefore was abandoned. Hence, as the matrix method was more accurate and complete, it was preferred over the simple method. Although it may be limited by the need for parameters that are currently difficult to obtain, such as the lens radii of curvature, new technologies are continuously being introduced that will help to overcome these issues. In the meantime, the simple method can provide a reliable first-order estimate.

Diabetes can affect the ocular components, particularly the aqueous humour and the lens, thereby producing changes in refractive error. In poorly controlled diabetes, fluctuations in the properties of the aqueous humour can rapidly impact internal refraction, leading to variations in vision. Additionally, diabetes can gradually affect the lens, potentially causing longer term changes in lens curvature.^{35,50}

In conclusion, this work proposed two methods for estimating the contribution of variations in ocular biometric components to the resulting refracting error within a population. About 50%–65% of these refractive error changes are determined by variations in axial length, and to a lesser degree by variations in lens and corneal power. The latter two appear to vary in importance, depending on the measuring equipment being used and the population being considered.

AUTHOR CONTRIBUTIONS

Arezoo Farzanfar: Conceptualization (lead); data curation (equal); formal analysis (equal); investigation (equal); methodology (equal); software (lead); validation (equal); writing – original draft (equal); writing – review and editing (equal). **Veronica Lockett-Ruiz:** Conceptualization (equal); investigation (equal); methodology (equal); resources (equal); writing – review and editing (equal). **Rafael Navarro:** Conceptualization (equal); investigation (equal); methodology (equal); supervision (equal); writing – review and editing (equal). **Carina Koppen:** Funding acquisition (equal); supervision (equal). **Jos J. Rozema:** Conceptualization (equal); funding acquisition (equal); investigation (equal); methodology (equal); project administration (equal);

supervision (equal); writing – original draft (equal); writing – review and editing (equal).

FUNDING INFORMATION


This project received funding from the European Union's Horizon 2020 research and innovation programme under the Marie Skłodowska Curie grant agreement No. 956720.

CONFLICT OF INTEREST STATEMENT

None.

ORCID

Arezoo Farzanfar  <https://orcid.org/0000-0002-0990-7800>

Veronica Lockett-Ruiz  <https://orcid.org/0000-0002-9413-838X>

Rafael Navarro  <https://orcid.org/0000-0002-1328-1716>

Carina Koppen  <https://orcid.org/0000-0002-7728-7260>

Jos J. Rozema  <https://orcid.org/0000-0001-8124-8646>

REFERENCES

- Olsen T, Arnarsson A, Sasaki H, Sasaki K, Jonasson F. On the ocular refractive components: the Reykjavik eye study. *Acta Ophthalmol.* 2007;85:361–6.
- Berg F. Über Variabilität und Korrelation bei den verschiedenen Abmessungen des Auges. *Graefes Arch Clin Exp Ophthalmol.* 1931;127:606–39.
- Strömberg E. XXXIV: Über Refraktion und Achsenlänge des menschlichen Auges: (Vorläufige Mitteilung). *Acta Ophthalmol.* 1936;14:281–97.
- Stenstrom S. Variations and correlations of the optical components of the eye. *Mod Trends Ophthalmol.* 1948;2:87–102.
- Benjamin B, Davey J, Sheridan M, Sorsby A, Tanner J. Emmetropia and its aberrations; a study in the correlation of the optical components of the eye. *Spec Rep Series Med Res Council (GB).* 1957;11:1–69.
- Fieß A, Nickels S, Schulz A, Münzel T, Wild PS, Beutel ME, et al. The relationship of ocular geometry with refractive error in normal and low birth weight adults. *J Optom.* 2021;14:50–7.
- Hou W, Norton TT, Hyman L, Gwiazda J, Group C. Axial elongation in myopic children and its association with myopia progression in the correction of myopia evaluation trial (COMET). *Eye Contact Lens.* 2018;44:248–59.
- Meng W, Butterworth J, Malecaze F, Calvas P. Axial length of myopia: a review of current research. *Ophthalmologica.* 2011;225:127–34.
- Shufelt C, Fraser-Bell S, Ying-Lai M, Torres M, Varma R. Refractive error, ocular biometry, and lens opalescence in an adult population: the Los Angeles Latino eye study. *Invest Ophthalmol Vis Sci.* 2005;46:4450–60.
- Mallen EA, Gammoh Y, Al-Bdour M, Sayegh FN. Refractive error and ocular biometry in Jordanian adults. *Ophthalmic Physiol Opt.* 2005;25:302–9.
- Hashemi H, Khabazkhoob M, Emamian MH, Shariati M, Miraftab M, Yekta A, et al. Association between refractive errors and ocular biometry in Iranian adults. *J Ophthalmic Vis Res.* 2015;10:214–20.
- McBrien NA, Adams DW. A longitudinal investigation of adult-onset and adult-progression of myopia in an occupational group. Refractive and biometric findings. *Invest Ophthalmol Vis Sci.* 1997;38:321–33.
- Yekta A, Fotouhi A, Hashemi H, Ostadi MH, Heravian J, Heydarian S, et al. Relationship between refractive errors and ocular biometry components in carpet weavers. *Iran J Ophthalmol.* 2010;22:45–54.
- Ojaimi E, Rose KA, Morgan IG, Smith W, Martin FJ, Kifley A, et al. Distribution of ocular biometric parameters and refraction in a

- population-based study of Australian children. *Invest Ophthalmol Vis Sci*. 2005;46:2748–54.
15. Warrier SK, Wu HM, Newland HS, Muecke JS, Selva D, Aung T, et al. Ocular biometry and determinants of refractive error in rural Myanmar: the Meiktila eye study. *Br J Ophthalmol*. 2008;92:1591–4.
 16. Wickremasinghe S, Foster PJ, Uranchimeg D, Lee PS, Devereux JG, Alsbirk PH, et al. Ocular biometry and refraction in Mongolian adults. *Invest Ophthalmol Vis Sci*. 2004;45:776–83.
 17. Rozema J, Dankert S, Iribarren R. Emmetropization and non-myopic eye growth. *Surv Ophthalmol*. 2023;68:759–83.
 18. Straub M. Über die Aetiologie der Brechungsanomalien des Auges und den Ursprung der Emmetropie. *Graefes Arch Ophthalmol*. 1909;70:130–99.
 19. Rozema JJ. Refractive development I: biometric changes during emmetropisation. *Ophthalmic Physiol Opt*. 2023;43:347–67.
 20. Mutti DO, Mitchell GL, Sinnott LT, Jones-Jordan LA, Moeschberger ML, Cotter SA, et al. Corneal and crystalline lens dimensions before and after myopia onset. *Optom Vis Sci*. 2012;89:251–62.
 21. Rozema J, Dankert S, Iribarren R, Lanca C, Saw S-M. Axial growth and lens power loss at myopia onset in Singaporean children. *Invest Ophthalmol Vis Sci*. 2019;60:3091–9.
 22. Rozema JJ, Tassignon M-J. The Bigaussian nature of ocular biometry. *Optom Vis Sci*. 2014;91:713–22.
 23. Steiger A. Die Entstehung der sphärischen Refraktionen des menschlichen Auges. S. Berlin: Karger; 1913.
 24. Flitcroft D. Emmetropisation and the aetiology of refractive errors. *Eye*. 2014;28:169–79.
 25. Norrby S. Sources of error in intraocular lens power calculation. *J Cataract Refract Surg*. 2008;34:368–76.
 26. Olsen T. Sources of error in intraocular lens power calculation. *J Cataract Refract Surg*. 1992;18:125–9.
 27. Hirschschall N, Findl O, Bayer N, Leisser C, Norrby S, Zimper E, et al. Sources of error in toric intraocular lens power calculation. *J Refract Surg*. 2020;36:646–52.
 28. Ribeiro F, Castanheira-Dinis A, Dias JM. Refractive error assessment: influence of different optical elements and current limits of biometric techniques. *J Refract Surg*. 2013;29:206–12.
 29. Navarro R, Lockett-Ruiz V, López JL. Analytical ray transfer matrix for the crystalline lens. *Biomed Opt Express*. 2022;13:5836–48.
 30. Rozema JJ, Rodriguez P, Navarro R, Tassignon M-J. SyntEyes: a higher-order statistical eye model for healthy eyes. *Invest Ophthalmol Vis Sci*. 2016;57:683–91.
 31. Mutti DO, Sinnott LT, Mitchell GL, Jordan LA, Friedman NE, Frane SL, et al. Ocular component development during infancy and early childhood. *Optom Vis Sci*. 2018;95:976–85.
 32. Twelker JD, Mitchell GL, Messer DH, Bhakta R, Jones LA, Mutti DO, et al. Children's ocular components and age, gender, and ethnicity. *Optom Vis Sci*. 2009;86:918–35.
 33. Rozema JJ, Herscovici Z, Snir M, Axer-Siegel R. Analysing the ocular biometry of new-born infants. *Ophthalmic Physiol Opt*. 2018;38:119–28.
 34. Cook A, White S, Batterbury M, Clark D. Ocular growth and refractive error development in premature infants with or without retinopathy of prematurity. *Invest Ophthalmol Vis Sci*. 2008;49:5199–207.
 35. Suheimat M, Efron N, Edwards K, Pritchard N, Mathur A, Mallen EA, et al. Biometry of eyes in type 1 diabetes. *Biomed Opt Express*. 2015;6:702–15.
 36. Gertsbakh I. Measurement uncertainty: error propagation formula. Measurement theory for engineers. Berlin: Springer; 2003. p. 87–94.
 37. Kuo W, Uppuluri V. A review of error propagation analysis in systems. *Microelectron Reliab*. 1983;23:235–48.
 38. Rozema JJ. Estimating principal plane positions for ocular power calculations in children and adults. *Ophthalmic Physiol Opt*. 2021;41:409–13.
 39. Yudkin AM. The formation of the aqueous humor: its relation to intra-ocular and vascular pressures. *Arch Ophthalmol*. 1929;1:435–46.
 40. Yudkin AM. The aqueous humor: a critical and experimental study. *JAMA*. 1926;87:1910–6.
 41. Evans T, Rubin A. Linear optics of the eye and optical systems: a review of methods and applications. *BMJ Open Ophthalmol*. 2022;7:e000932. <https://doi.org/10.1136/bmjophth-2021-000932>
 42. O'Brien C, Clark D. Ocular biometry in pre-term infants without retinopathy of prematurity. *Eye*. 1994;8:662–5.
 43. Bennett A. A method of determining the equivalent powers of the eye and its crystalline lens without resort to phakometry. *Ophthalmic Physiol Opt*. 1988;8:53–9.
 44. Rozema JJ, Atchison DA, Tassignon M-J. Comparing methods to estimate the human lens power. *Invest Ophthalmol Vis Sci*. 2011;52:7937–42.
 45. Axer-Siegel R, Bourla D, Sirota L, Weinberger D, Snir M. Ocular growth in premature infants conceived by in vitro fertilization versus natural conception. *Invest Ophthalmol Vis Sci*. 2005;46:1163–9.
 46. Navarro R, Santamaria J, Bescós J. Accommodation-dependent model of the human eye with aspherics. *J Opt Soc Am A*. 1985;2:1273–80.
 47. Fledelius HC, Fledelius C. Eye size in threshold retinopathy of prematurity, based on a Danish preterm infant series: early axial eye growth, pre-and postnatal aspects. *Invest Ophthalmol Vis Sci*. 2012;53:4177–84.
 48. Bhatti S, Paysse EA, Weikert MP, Kong L. Evaluation of structural contributors in myopic eyes of preterm and full-term children. *Graefes Arch Clin Exp Ophthalmol*. 2016;254:957–62.
 49. Kaur S, Dogra M, Sukhija J, Samanta R, Singh SR, Grover S, et al. Preterm refraction and ocular biometry in children with and without retinopathy of prematurity in the first year of life. *J Am Assoc Pediat Ophthalmol Strab*. 2021;25:271.e1–271.e6.
 50. Rozema JJ, Khan A, Atchison DA. Modelling ocular ageing in adults with well-controlled type I diabetes. *Adv Ophthalmol Pract Res*. 2022;2:100048. <https://doi.org/10.1016/j.aopr.2022.100048>
 51. Kaštelan S, Gverović-Antunica A, Peščić G, Gotovac M, Marković I, Kasun B. Refractive changes associated with diabetes mellitus. *Semin Ophthalmol*. 2018;33:838–84.
 52. Sorsby A, Benjamin B, Bennett AG. Steiger on refraction: a reappraisal. *Br J Ophthalmol*. 1981;65:805–11.
 53. Hirsch MJ, Weymouth FW. Notes on ametropia—a further analysis of Stenström's data. *Optom Vis Sci*. 1947;24:601–8.
 54. Olsen T. On the calculation of power from curvature of the cornea. *Br J Ophthalmol*. 1986;70:152–4.
 55. Ho J-D, Tsai C-Y, Tsai R-J-F, Kuo L-L, Tsai I-L, Liou S-W. Validity of the keratometric index: evaluation by the Pentacam rotating Scheimpflug camera. *J Cataract Refract Surg*. 2008;34:137–45.

SUPPORTING INFORMATION

Additional supporting information can be found online in the Supporting Information section at the end of this article.

How to cite this article: Farzanfar A, Lockett-Ruiz V, Navarro R, Koppen C, Rozema JJ. The influence of variations in ocular biometric and optical parameters on differences in refractive error. *Ophthalmic Physiol Opt*. 2024;00:1–10. <https://doi.org/10.1111/opo.13318>